7-2013

Dual-Carrier High-Gain Low-Noise Superlattice Avalanche Photodiodes

Jun Huang

Koushik Banerjee

Siddhartha Ghosh

Majeed M. Hayat

IEEE Transactions on Electron Devices, Vol. 60, No. 7 (July 2013): 2296-2301. DOI.

Dual-Carrier High-Gain Low-Noise Superlattice Avalanche Photodiodes

Jun Huang
Lab for Photonics and Magnetics (ECE Department), University of Illinois at Chicago, Chicago, IL
Koushik Banerjee
Intel Corporation, Santa Clara, CA
Siddhartha Ghosh
Lab for Photonics and Magnetics (ECE Department), University of Illinois at Chicago, Chicago, IL
Majeed M. Hayat
Center for High Technology Materials and the ECE Dept, University of New Mexico, Albuquerque, NM

Abstract:

In this paper, novel avalanche photodiode structures with alternate carrier multiplication nanometer regions, placed next to a wider electron multiplication region, to create dual-carrier feedback systems, are proposed. Gain and excess noise factor of these structures are calculated based on the dead space multiplication theory

under uniform electric field. In addition, the equivalent impact ionization ratios are derived and compared. It is observed that the proposed structures can generate much higher gain compared with conventional pure electron multiplication structures under the same electric field without severely degrading the excess noise quality. Excess noise is further optimized with careful adjustment of thin multiplication regions' thicknesses. These high-gain structures can operate under low-bias (<; 5 V) conditions, making it possible to integrate infrared avalanche photodiodes (APDs) directly into silicon read-out circuits. In this paper, type-II mid-wavelength infrared InAs/GaSb strained layer superlattice is used for simulation. However, the concept of dual-carrier APDs, with carrier feedback to generate high gain and control of excess noise through confining impact ionization in thin layers, is general and can also be applied to other wavelength APDs with different materials and thicknesses. Type II InAs/GaSb strain layer superlattice allows for versatile band structure design leading to impact ionization coefficient engineering.

SECTION I. Introduction

Avalanche photodiodes (APDs), which have signal amplification combined with light detection in a single stage, are often used for infrared devices. They operate at a relatively high reverse bias to enable avalanche multiplication from the cascade of impact ionization of electrons and holes. However, the multiplication process introduces noise as a result of randomness in the spatial location at which secondary carriers are generated, as well as accompanying randomness in the total number of carriers produced per initial photogenerated carrier. This noise is known as the excess noise, which is characterized by the excess noise factor F [1], [2]. McIntyre [3] first quantified the excess noise factor. Based on [1], excess noise is a function of the ratio of the hole-to-electron ionization coefficients k. The excess noise factor can be minimized with k approaching zero or infinity, which indicates a single-carrier multiplication process (electron or hole, respectively). Significant efforts are put to achieve single carrier dominated multiplication using mercury cadmium telluride [4] and III–V type II strained layer InAs/GaSb superlattice [5], [6]. However, single carrier multiplication eliminates or reduces multiplication by the second type of carrier, resulting in a lower gain with the same multiplication region width and the same electric field. Thus, it requires much higher electric fields to achieve the same gain as a double carrier multiplication device. Further, high electric field can significantly increase dark currents, both surface leakage and tunneling currents, which can limit the performance of APDs instead of the excess noise factor. The problem becomes severe with narrow bandgap materials that are used for longer wavelength infrared detection. Higher bias requirements also pose a compatibility problem with silicon readout circuits that normally operate under low bias values. In addition, in single-photon counting applications, APDs require higher overbias in the linear mode and they become susceptible to higher dark count rates.

Until now, many efforts are put on new materials based on separate absorption and multiplication (SAM) structures. In this paper, we examine novel structures that also have separated absorption and multiplication regions; however, they have alternate carrier (electron or hole) multiplication regions arranged in thin layers, judiciously combined together to form that multiplication region. By simply adding thin carrier multiplication layers to conventional pure electron multiplication structures, novel APD designs can be generated, in which gain and excess noise can be tuned by changing the material composition of layer structures along with the thickness of each thin layer. This kind of structure aims to achieve extremely high gain at a lower bias while the excess noise is kept at a relatively low level. In addition, this kind of structure can be applicable to a broader choice of materials. Different materials and layer thicknesses can be applied depending on the mode of operation, target wavelength, and specific application needs.

The analytic dead space multiplication theory, which has an effective performance prediction for thin APDs, is applied in this paper to simulate these structures.

SECTION II. Dead Space Multiplication Theory for Gain and Excess Noise

We begin by reviewing some important notes of the dead space multiplication theory. The minimum distance that a newly generated carrier must travel to acquire threshold energy is called the carrier dead space [7]. The electron and hole dead space, denoted by d_{e} and d_{h}, respectively, are given by [7] the following:

$$d_{\mathrm{e}} = \frac{E_{\mathrm{ie}}}{q\varepsilon}$$
$$d_{\mathrm{h}} = \frac{E_{\mathrm{ih}}}{q\varepsilon} \quad (1)(2)$$

where q is the electronic charge, ε is the uniform electric field in the multiplication region, E_{ie} and E_{ih} are the ionization threshold energies of the electron and hole, respectively. To be more specific, for a single multiplication region with the same threshold energy, (1) and (2) are enough. However, when it is applied to several thin multiplication regions with different threshold energies, dead space for electrons and holes around the boundaries should be modified. This will be discussed later in this paper.

Consider a multiplication region that extends from $x = 0$ to $x = W$, and the direction of electric field points from $x = W$ to $x = 0$. The gain and excess noise factor were reported in [8] under uniform electric field and then extended in [9] to nonuniform electric fields. We will review germane aspects of the model briefly. Following [8], a random sum $Z(x)$ is defined as the overall electrons and holes generated by a single parent electron. Similarly, $Y(x)$ is the random number of all electrons and holes produced by a single parent hole. For the case of electron injection, since $Y(0) = 1$, the random gain of the device, G, which is given by $G = (1/2)(Z(0) + Y(0))$, can be reduced to $G = (1/2)(Z(0) + 1)$. According to [9], (4) and (5), the average of $Z(x)$ and $Y(x)$, denoted by $z(x)$ and $y(x)$ can be obtained by the following:

$$z(x) = \left[1 - \int_{-\infty}^{W-x} h_{\mathrm{e}}(x,\xi)d\xi\right] + \int_{x}^{W} [2z(\xi) + y(\xi)] \cdot h_{\mathrm{e}}(x,\xi - x)d\xi \quad (3)$$

and

$$y(x) = \left[1 - \int_{-\infty}^{x} h_{\mathrm{h}}(x,\xi)d\xi\right] + \int_{0}^{x} [2y(\xi) + z(\xi)] \cdot h_{\mathrm{h}}(x,x - \xi)d\xi \quad (4)$$

where h_{e} and h_{h} are the probability density functions (p.d.f.'s) of the random free-path lengths of the electron and hole, respectively. The p.d.f.s take the following form [9, eqs. (1a) and (1b)]:

$$h_{\mathrm{e}}(x,\eta) = \begin{cases} 0, \eta < d_{\mathrm{e}}(x) \\ \alpha(\eta + x)e^{-\int_{d_{\mathrm{e}}(x)}^{\eta} \alpha(x+\sigma)d\sigma}, d_{\mathrm{e}}(x) \le \eta \le W - x \end{cases} \quad (5a)(5b)$$
$$h_{\mathrm{h}}(x,\eta) = \begin{cases} 0, \eta < d_{\mathrm{h}}(x) \\ \beta(x - \eta)e^{-\int_{d_{\mathrm{h}}(x)}^{\eta} \beta(x-\sigma)d\sigma}, d_{\mathrm{h}}(x) \le \eta \le x \end{cases}$$

where $\alpha(y)$ is the ionization probability density of the electron that may ionize at location $y \in [x + d_{\mathrm{e}}(x), W]$ after it travels without ionizing a distance $d_{\mathrm{e}}(x)$. Similarly, $\beta(y)$ is the ionization probability density of

the hole that may ionize at location $y \in [0, x - d_{\mathrm{h}}(x)]$ after it travels in an opposite direction without ionizing a distance $d_{\mathrm{h}}(x)$. Thus, the mean gain $\langle G \rangle$ can be obtained as follows:

$$\langle G \rangle = \frac{1}{2}[z(0) + 1] \quad (6)$$

while the excess noise factor, F, is given by [8, eq. (11)]

$$F = \frac{\langle G^2 \rangle}{\langle G \rangle^2} = \frac{z_2(0)+2z(0)+1}{(z(0)+1)^2} \quad (7)$$

where $z_2(x)$ is the second moment of $Z(x)$. For $0 < x < W$, it can be described as follows:

$$\begin{aligned} z_2(x) = \; & \langle Z^2(x) \rangle \\ = \; & [1 - \int_{-\infty}^{W-x} h_{\mathrm{e}}(x, \xi) d\xi] \\ & + \int_0^x [2z_2(\xi) + y_2(\xi) + 4z(\xi)y(\xi) + 2z^2(\xi)] \\ & \cdot h_{\mathrm{e}}(x, \xi - x) d\xi \end{aligned} \quad (8)$$

and $y_2(x)$ is the second moment of $Y(x)$, determined as follows:

$$\begin{aligned} y_2(x) = \; & \langle Y^2(x) \rangle \\ = \; & [1 - \int_{-\infty}^{W-x} h_{\mathrm{h}}(x, \xi) d\xi] \\ & + \int_0^x [2y_2(\xi) + z_2(\xi) + 4z(\xi)y(\xi) + 2y^2(\xi)] \\ & \cdot h_{\mathrm{h}}(x, \xi - x) d\xi \end{aligned} \quad (9)$$

while at $x = W$

$$z_2(W) = 1 \quad (10)$$

and at $x = 0$

$$y_2(W) = 1. \quad (11)$$

The mean gain and the excess noise factor can be estimated by solving the recurrence (3), (4), (8), and (9) using iterative numerical method.

SECTION III. Novel Structures and Application of Dead Space Multiplication Theory

An APD with conventional SAM structure is shown in Fig. 1(a). To show the structure, area absorption denotes Superlattices structure region for absorber, electron multiplication for electron multiplication region.

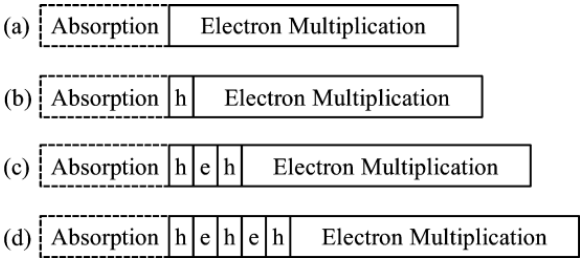

Fig. 1. Four structures with different multiplication regions. (a) Single carrier (electron) multiplication. (b)–(d) Dual carrier multiplication structures with 10-nm hole multiplication layer, 800-nm electron multiplication layer, and 10-nm electron multiplication layer, respectively.

The proposed device structure is shown in Fig. 1(b) which also contains the absorber and electron multiplication region. A thin hole multiplication region noted by h is inserted between absorber and electron multiplication regions in this device structure. Electron and hole multiplication regions are implemented using type-II SLS materials used previously in electron-[5] and hole-[6] APDs. The design implemented with above materials ensures that only electrons initiate the avalanching process in the electron-multiplication region and holes in the hole-multiplication region.

We assume that the electric field extends from area electron multiplication to area absorption in both structures (a) and (b). In structure (a), electron-hole pairs are created from electron impact ionizations. Secondary electrons may also get impact ionized as long as they travel farther than their dead-space distance, acquiring energy in excess of than ionization threshold energy. However, the secondary holes will leave the multiplication region without any impact ionization as the material in this region is bandstructure engineered to have pure electron multiplication. Nonetheless, in structure (b), when the secondary holes travel through the thin hole multiplication region h, they also have the possibility to impact ionize as this region is designed for hole multiplication. Thus, extra electron-hole pairs are created compared with structure (a). In addition, the secondary electrons created in region h, that are drifted into electron multiplication region by electric field, can also impact ionize. This results in additional electron-hole pairs and also allows newly created holes to impact ionize again in region h. Therefore, a dual-carrier feedback system is created and higher gain can be expected as many more electron-and-hole pairs are generated.

Further, for structures in Fig. 1(c) and (d), with more thin layers alternatively added, larger gain can be expected not only because the hole impact ionization possibility increases, but also more feedback paths are created.

To simulate gain and excess noise, it is necessary to determine dead spaces (d_{e} and d_{h}) for electrons and holes. For a certain uniform electric field, the ionization threshold energies were assumed to be equal to their bandgaps and ionization coefficients were extracted from experimental gain variation with bias from [5] and [6].

However, when two or more thin multiplication regions are present, dead spaces for carriers within a distance less than dead space to the boundaries between two thin multiplication regions should be modified.

For example, if one electron is generated at a position ($x = x'$) with a distance ξ' to the boundary ($x = b$), and under electric field it drifts toward the boundary. If ξ' is large enough, it can get impact ionized after it travels a dead space distance in this region. The dead space $d_{\mathrm{e}}(x')$ is described as $d_{\mathrm{e}}(x') = d_{\mathrm{e1}} = E_{\mathrm{ie1}}/q\varepsilon$, where q is the electronic charge, ε is the uniform electric field, and E_{ie1} are the ionization threshold energy of the electron in its original multiplication region.

However, if ξ' is less than its dead space d_{e1}, the electron will reach the boundary without ionization. Thus, when this electron enters into the second region, it carries a kinetic energy, $E'_{\mathrm{e}} = q\varepsilon\xi'$, which describes the energy of this electron that accumulates under electric field ε drifting with a distance ξ'. If E'_{e} is larger than the threshold energy E_{ie2} for electron in the second region, the electron will impact ionize immediately. If it is smaller, the electron still has to travel with a distance to achieve the threshold energy for electrons in the second region. Therefore, under the condition of $\xi' < d_{\mathrm{e1}}$, the dead space of this electron can be modified as follows:

$$d_{\mathrm{e}}(x') = \begin{cases} \xi', E'_{\mathrm{e}} \geq E_{\mathrm{ie2}} \\ \xi' + \frac{E_{\mathrm{ie2}} - E'_{\mathrm{e}}}{q\varepsilon}, E'_{\mathrm{e}} < E_{\mathrm{ie2}} \end{cases} \quad (12)$$

where q is the electronic charge, ε is the uniform electric field, E_{ie2} are the ionization threshold energy of the electron in second multiplication region, and E'_{e} is the initial energy of electron when it enters into the second regions.

Similarly, for a hole generated at a position $(x = x')$ with a distance ξ'' to the boundary $(x = c)$ where ξ'' is less than dead space d_{h1} and under electric field it drifts to the boundary, in its original region, the dead space can be modified as follows:

$$d_{\mathrm{h}}(x') = \begin{cases} \xi'', E'_{\mathrm{h}} \geq E_{\mathrm{ih2}} \\ \xi'' + \frac{E_{\mathrm{ih2}} - E'_{\mathrm{h}}}{q\varepsilon}, E'_{\mathrm{h}} < E_{\mathrm{ih2}} \end{cases} \quad (13)$$

where q is the electronic charge, ε is the uniform electric field, E_{ih2} are the ionization threshold energies of the electron in second multiplication region, and E'_{h} is the initial energy of hole when it enters into the second regions.

Now according to the dead-space multiplication theory, the excess noise factor is a function of the ionization coefficient ratio and the mean gain, as well as the multiplication-region width. The thickness of thin hole-multiplication region h is set to be thinner than the hole's dead space distance. This restriction in the multiplication width ensures that only those carriers that gain sufficient energy prior to entering the thin region can impact ionize. The structure does not provide enough distance for secondary carriers to buildup their energy to the threshold-energy level. This reduces the randomness of ionization (position randomness) for holes, hence to minimize the excess noise factor. Dead spaces calculated for holes in hole multiplication region and electrons in electron multiplication region are ~170 and 107 nm, respectively, at an electric field of 20 kV/cm. Thus, thicknesses are 10 nm which is almost one tenth of its dead space for thin hole multiplication region h, 10 nm for thin electron multiplication region e and 800 nm for wide electron multiplication region electron multiplication.

SECTION IV. Results and Discussion

Variations of the mean gain with applied electric field for the different structures are shown in Fig. 2. The results highlight the increase of multiplication gain through higher carrier feedback generated in additional thin multiplication regions. To be more specific, to achieve a gain of 40, only a bias of 2.1 V needs to be applied to structure (d) instead of 17.6 V to structure (a). Thus, the required bias is reduced by almost eight times at this gain. As previously stated, high bias can increase dark currents, especially for long wave infrared devices. Thus, these new structures [from structure (b) to (d)] have a positive effect on dark current reduction. In addition, they can be potentially used for low-bias high-gain applications, such as single photon counting devices that can be directly integrated to Si readout circuits which operate at a relatively low voltage.

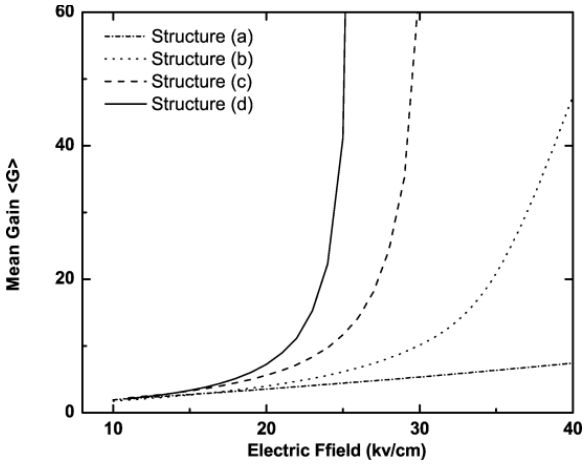

Fig. 2. Comparison of different mean gain ⟨G⟩ with the variation of electric field across four structures (a)–(d). A uniform electric field is assumed through all four structures.

From a different perspective, the additional gain from the thin multiplication layers can be traded for a lower thickness of the wider electron multiplication region. To study the effectiveness on the thickness reduction, thickness of the whole multiplication versus gain is shown in Fig. 3. It is shown that under an electric field of 20 kV/cm, with only adding five thin 10-nm alternate carrier multiplication layers from structure (a) to (d), the thickness can be reduced from 1840 to 1009 nm at a mean gain of 20, which enables us to fabricate APD devices with smaller size. Variations of excess noise factors versus mean gain for the different structures are shown in Fig. 4. Structure (a), comprised of a single almost pure electron multiplication region, has the least excess noise as expected from McIntyre model. It is clearly seen from the slopes of four curves that the increase in excess noise with gain is progressively steeper from structure (a) to structure (d). To better understand and control the excess noise factor in the proposed dual-carrier APD structure, the overall equivalent impact ionization coefficient ratio k_{equiv} is calculated with variable thickness of the thin carrier multiplication region in Fig. 5 k_{equiv} can be determined by using the conventional expression for the excess noise factor [2]

$$F = k\langle G\rangle + (1-k)\left(2 - \frac{1}{\langle G\rangle}\right). \quad (14)$$

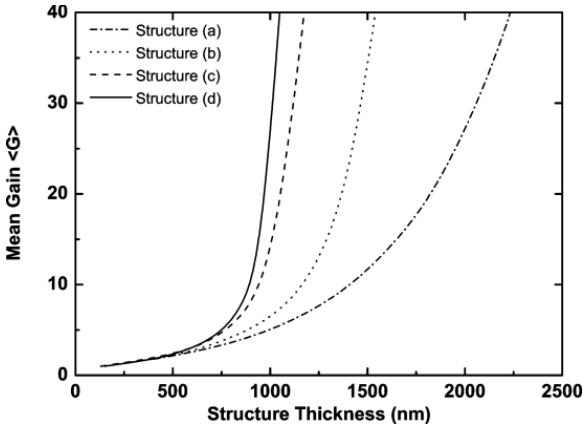

Fig. 3. Comparison of the DSMT-simulated structure thicknesses as a function of mean gain ⟨G⟩ for all four structures.

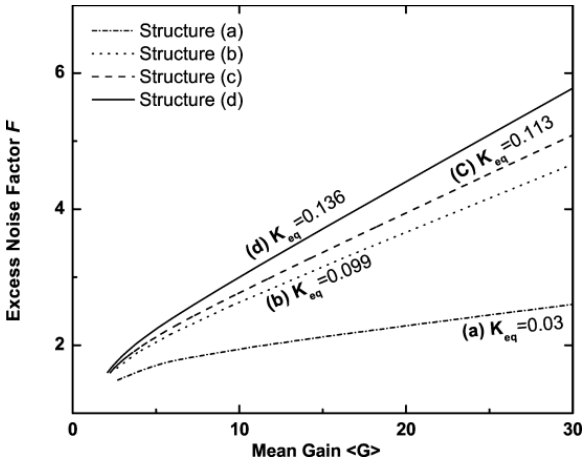

Fig. 4. Comparison of the DSMT-computed excess noise factors F for structures (a)–(d) as a function of mean gain $\langle G \rangle$.

Hence, if the overall mean gain $\langle G \rangle$ and excess noise factor F are known, Keq can be calculated as follows:

$$k_{\text{equiv}} = \frac{F-(2-\frac{1}{\langle G \rangle})}{\langle G \rangle+\frac{1}{\langle G \rangle}-2}. \quad (15)$$

Simulations are performed with an electric field of 20 kV/cm with a dead space of 107 and 170 nm for hole and electron multiplication. Width of thin region is changed while keeping total width the same. It is known that the impact ionization coefficient ratio is 0.03 [5] in structure (a) as it only has electron multiplication region.
In Fig. 5, k_{eq} of the different structures are compared with variable thin region width. For a thickness of 10-nm structures (b), (c), and (d) have k_{equiv} of 0.099, 0.113, and 0.136, respectively, which are higher compared with structure (a). In addition, for each structure in Fig. 5, k_{equiv} increases with thickness of each thin multiplication region, which is in accord with the design rule of this dual APD structure that thinner hole multiplication region decreases position randomness of impact ionization, therefore, reducing the excess noise [10]. Thus, to obtain a lower excess noise, thickness of thin multiplication regions must be minimized. However, gain decreases with that thickness as well. Therefore, there is a tradeoff between gain and excess noise. Specific region thickness and materials used for this model can be selected to satisfy specific design requirements.

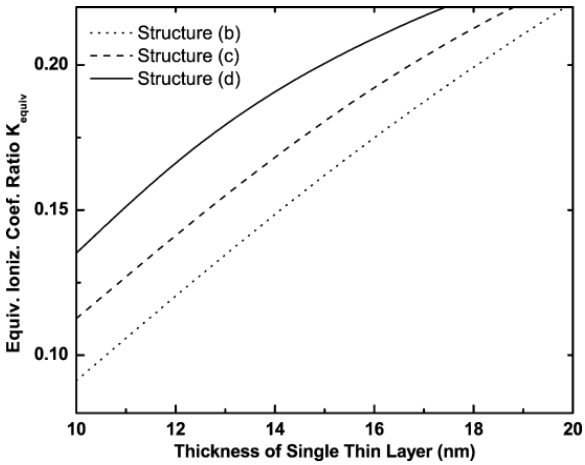

Fig. 5. Comparison of the DSMT-simulated equivalent ionization coefficient ratios k_{equiv} for structures (b)–(d) as a function of thickness of single thin multiplication region layer.

Finally, for these dual-carrier structures, based on the role of carrier heating in avalanche multiplication (also termed the initial-energy effect) reported in [11] in the context of a very low-noise GaAs-based APD developed by Campbell et al., it was obvious that only heated holes from the wider electron multiplication region can impact ionize inside the thin multiplication region and the secondary carriers generated inside do not. Therefore, as long as the hole impact ionization rates in the thin hole-multiplication region stays the same, the overall excess noise factors will not be affected no matter what the electron impact ionization rate is in that region since electrons in that thin region are either generated inside or from other thin regions that is not heated enough. This is confirmed by simulation results shown in Fig. 6. The overall excess noise factor versus mean gain in structure (d) is simulated by keeping the hole impact ionization rate in the thin hole multiplication region the same while changing the electron impact ionization rates in that region that makes the impact ionization coefficient ratio k's in the thin hole multiplication region different. The same excess noise factor is achieved at the same gain with different k's. Two typical k's ($k' = 0$ and $k' = 1$) are selected to be shown in Fig. 6. This observation provides greater flexibility in making a suitable choice for thin region materials, as only the value of the hole ionization coefficient needs to be considered without regarding the same for electron ionization inside the thin region.

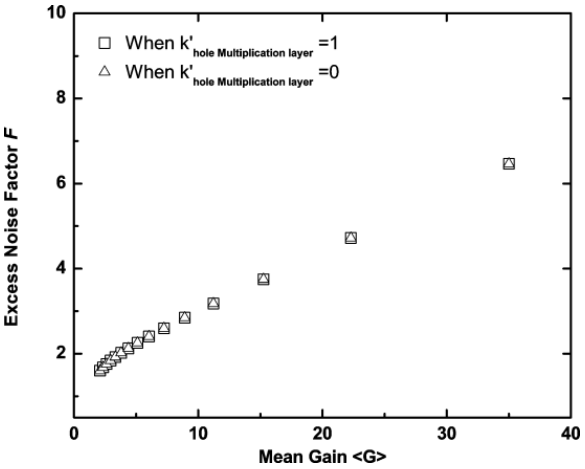

Fig. 6. Variation of excess noise factor F with mean gain $\langle G \rangle$ for structure (d) when impact ionization ratio (k') in thin hole multiplication region (h) is changed to either 0 or 1. For these two situations, the same excess noise factor is achieved with the same gain. This illustrates that the ionization coefficient ratio within the hole multiplication region does not affect the overall excess noise factor.

SECTION V. Conclusion

New dual-carrier feedback APD structures were proposed in this paper. Unlike normal SAM structures with only one multiplication region, these structures use one or multiple thin alternate hole multiplication layers placed adjacent to a wide electron multiplication region. This created dual carrier feedback through controlled carrier multiplication inside thin layers. A specifically lattice engineered type-II SLS was used as the electron multiplication region while the thin hole multiplication region was composed of $\mathrm{In}_x\mathrm{Ga}_{1-x}\mathrm{Sb}$. Simulations were carried out to predict the performance using the dead space multiplication theory. The device design allowed the APDs to have higher gains in exchange of a controlled tradeoff with excess noise. Gains much higher than a single carrier APS, were achieved under a relatively low bias ($< 5V$), which created the possibility of integrating dual APDs directly to silicon read-out circuits without the need of high voltage supplies. In addition, with low electric field, it can reduce dark currents in linear and dark count and afterpulsing in single photon counting applications. The width of the thin region was shown to be the most critical parameter determining the device performance. With that width increasing, both gain and excess noise increase. For its frequency response, as this

APD structure employed both electrons and holes to create feedback systems, there will be a reduction in bandwidth, thus resulting in low gain-bandwidth products.

It was emphasized that these structures were novel SAM structures that combine both the hole and electron multiplication regions in different physical locations which created new gain-and-excess-noise characteristics. Although the current discussion involved only mid wavelength infrared APDs based on III–V SLS, it can be extended to other material systems where two different regions can be grown together with different carriers dominating the avalanching process. Material properties such as bandgap, ionization coefficients, and band alignments need careful selection to satisfy specific application requirements.

References

1. M. C. Teich, K. Matsuo, B. E. A. Saleh, "Excess noise factors for conventional and superlattice avalanche photodiodes and photomultiplier tubes", *IEEE J. Quantum Electron.*, vol. 22, pp. 1184-1193, Aug. 1986.

2. B. E. A. Saleh, M. C. Teich, "17" in Fundamentals of Photonics, USA, NY, New York:Wiley, 1991.

3. R. J. McIntyre, "Multiplication noise in uniform avalanche diodes", *IEEE Trans. Electron Devices*, vol. 13, pp. 164-168, Jan. 1966.

4. M. A. Kinch, J. D. Beck, C.-F. Wan, F. Ma, J. Campbell, "HgCdTe electron avalanche photodiodes", *J. Electronic Mat.*, vol. 33, pp. 630-639, Jun. 2004.

5. S. Mallick, K. Banerjee, J. B. Rodriguez, S. Krishna, S. Ghosh, "Ultralow noise midwave infrared InAs–GaSb strain layer superlattice avalanche photodiode", *Appl. Phys. Lett.*, vol. 91, no. 24, pp. 241111-241113, Dec. 2007.

6. K. Banerjee, S. Ghosh, S. Mallick, E. Plis, S. Krishna, C. Grein, "Midwave infrared InAs/GaSb strained layer superlattice hole avalanche photodiode", *Appl. Phys. Lett.*, vol. 94, no. 20, pp. 201107-201109, May 2009.

7. Y. Okuto, C. R. Crowell, "Ionization coefficients in semiconductors: A nonlocalized property", *Phys. Rev. B*, vol. 10, no. 10, pp. 4284-4296, 1974.

8. M. M. Hayat, B. E. A. Saleh, M. C. Teich, "Effect of dead space on gain and noise of double-carrier multiplication avalanche photodiodes", *IEEE Trans. Electron Devices*, vol. 39, pp. 546-552, Mar. 1992.

9. M. M. Hayat, W. L. Sargeant, B. E. Saleh, "Effect of dead space on gain and noise in Si and GaAs avalanche photodiodes", *IEEE J. Quantum Electron.*, vol. 28, pp. 1360-1365, May 1992.

10. M. A. Saleh, M. M. Hayat, B. E. A. Saleh, M. C. Teich, "Dead-space-based theory correctly predicts excess noise factor for thin GaAs and AlGaAs avalanche photodiodes", *IEEE Trans. Electron Devices*, vol. 47, pp. 625-633, Mar. 2000.

11. M. M. Hayat, O.-H. Kwon, S. Wang, J. C. Campbell, B. E. A. Saleh, M. C. Teich, " Boundary effects on multiplication noise in thin heterostructure avalanche photodiodes: Theory and experiment \$[{rm Al}_{0.6}{rm Ga}_{0.4}{rm As/GaAs}]\$ ", *IEEE Trans. Electron Devices*, vol. 49, pp. 2114-2123, Dec. 2002.